Two-dimensional to three-dimensional structural transition of gold cluster Au10 during soft landing on TiO2 surface and its effect on CO oxidation

Hui Li, Yong Pei, and Xiao Cheng Zeng

Citation: J. Chem. Phys. **133**, 134707 (2010); doi: 10.1063/1.3485291
View online: http://dx.doi.org/10.1063/1.3485291
View Table of Contents: http://jcp.aip.org/resource/1/JCPSA6/v133/i13
Published by the American Institute of Physics.

Two-dimensional to three-dimensional structural transition of gold cluster Au_{10} during soft landing on TiO_2 surface and its effect on CO oxidation

Hui Li, Yong Pei, and Xiao Cheng Zeng[a)]
Department of Chemistry and Nebraska Center for Materials and Nanoscience, University of Nebraska-Lincoln, Lincoln, Nebraska 68588, USA

(Received 21 June 2010; accepted 11 August 2010; published online 6 October 2010)

We investigate the possible structural transition of a planar Au_{10} cluster during its soft landing on a TiO_2 (110) surface with or with no oxygen defects. The collision between the gold cluster and the oxide surface is simulated using the Car–Parrinello quantum molecular dynamics method. Both high-speed and low-speed conditions typically implemented in soft-landing experiments are simulated. It is found that under a high-speed condition, the gold cluster Au_{10} can undergo a sequence of structural transitions after colliding with a defect-free TiO_2 (110) surface. When the TiO_2 (110) surface possesses oxygen vacancies, however, chemical bonds can form between gold and Ti atoms if gold atoms contact directly with the vacancies. As a consequence, one oxygen vacancy is capable of trapping one Au atom, and thus can split the Au_{10} into two parts while bouncing back from the surface. In addition, we study reaction pathways for the CO oxidation based on three isomer structures of Au_{10} observed in the soft-landing simulation: (1) the precollision two-dimensional structure, (2) a postcollision three-dimensional (3D) structure, and (3) an intermediate (transient) 3D structure that appeared in the midst of the collision. This study allows us to examine the structure-activity relationship using the Au_{10} as a prototype model catalyst. [doi:10.1063/1.3485291]

I. INTRODUCTION

Bulk gold is known to be inert to many chemical reactions. Gold clusters, however, exhibit exceptional catalytic activities in a number of important chemical reactions, such as CO oxidation, hydrogenation, dehydrogenation, and selective oxidation.[1–7] Previous studies have shown that catalytic capability of gold clusters can be affected by a number of factors, in particular the size and shape of the clusters. Indeed, gold clusters with different size and shape can have quite different electronic structures and local coordination of active sites,[8,9] thereby different reaction barriers to chemical reactions. Hence, it is important to understand the structure-activity relationship of gold clusters. Another important factor relevant to the catalytic activity is the interaction between a gold cluster and its support.[8,9] Very high activities for CO oxidation have been reported when Au clusters are supported by a metal oxide surface, for example, the TiO_2, Fe_2O_3, CeO_2, or MgO.[2,8,10–14] This support can significantly enhance their catalytic activities through several different ways, such as through the quantum size effect,[8] a charge transfer from defects,[15] or by strains due to the structural mismatch between Au clusters and the supports.[16] Nørskov and coworkers showed that low-coordinated Au sites are essential to the reactivity.[17,18] They used a three-dimensional (3D) Au_{10} cluster as a prototype model system and demonstrated that the small-sized Au_{10} is capable of catalyzing the CO oxidation below room temperature, even without the TiO_2 support.[19]

Since the catalytic activity can be strongly dependent on the structure of Au clusters, deposition conditions on a support (even the support is inert) may affect the final morphology of Au clusters and their activities.[20] In typical soft-landing experiments of metal clusters on a support, the gas-phase clusters are initially generated by laser vaporization, followed by mass selection through a mass spectrometer, before deposited on the support.[21] The speed of metal clusters can be lowered by the mass spectrometer prior to their landing on the support, which is a commonly used technique to avert cluster fragmentation during the collision.[21,22] Even under the "soft-landing" condition, the speed of metal clusters can still be on the order of hundreds or even thousands meters per second. Therefore, the collision between metal clusters and the support can still cause structural deformation and even structural transition. For gold clusters, the deformation and structural transition will likely affect their catalytic properties, even on an inert support.

Thus far, most previous theoretical studies of gold clusters supported by an oxide surface[4–19] have focused on geometric structure and electronic structure of the system, charge transfer to the support, as well as the chemical reaction pathways for the CO oxidation close to the interface between the clusters and the support. To our knowledge, the dynamic behavior of the gold clusters under soft-landing conditions and its effect on the structure-activity relationship before and after the landing have not been systematically studied. Here, we employed the Car–Parrinello molecular dynamics (CPMD) method to investigate the dynamics of a model gold cluster colliding with a TiO_2 support under two experimental soft-landing (speed) conditions. Particular at-

a)Author to whom correspondence should be addressed. Electronic mail: xzeng1@unl.edu.

tention is placed on effects of initial kinetic energy of the clusters, initial orientation of the clusters with respect to the support, and the oxygen vacancy on the dynamics of the clusters. We note that classic molecular dynamics (MD) simulations have been previously used to study collision between clusters and various surfaces,[23–25] for example, the landing of C_{60} molecules on graphite.[25] However, due to the lack of highly accurate potential functions for the Au–TiO_2 interaction, the classical MD simulation cannot realistically simulate the collision process between Au clusters and the TiO_2 support, particularly when bond-forming and bond-breaking are involved. On the other hand, in the CPMD simulation, forces between Au clusters and the TiO_2 support can be determined "on the fly" so that the dynamic behavior of the collision process can be simulated realistically.[26] More importantly, the bond-breaking and bond-making between the cluster and support or within the cluster can be taken into account in the CPMD simulation.[27] Nevertheless, the electronic structure calculation involved in the CPMD simulation is much more time consuming compared to the classical MD, particularly for relatively large system as considered here, which involves both a metal cluster and an oxide support. Fortunately, the time scale for the collision process is typically less than 1 ps, which is within the realm of the CPMD simulation.

In this study, the Au_{10} cluster is chosen as a prototype model system because of its exceptional catalytic activity.[18,19] The Au_{10}^- cluster anion has been shown to exhibit rich low-lying two-dimensional (2D) structures, both theoretically[28–31] and experimentally.[30,31] For neutral Au_{10}, previous theoretical studies have predicted that a 2D D_{2h} isomer is most likely the global minimum but a 3D isomer is energetically very competitive.[28,29] So there is a strong possibility of observing a collision-induced structural transition from 2D Au_{10}^- to 3D Au_{10} when the charge is transferred to the support. In this study, the TiO_2 (110) surface is considered as the support. In addition, the oxygen reduced TiO_2 surface[7] is considered to assess the effect of oxygen vacancy on the dynamic behavior of the gold cluster during the collision. Finally, we study the catalytic properties of the Au_{10} in three different isomeric structures which correspond to the isomer before, during, and after the collision with the TiO_2 surface. We use the CO oxidation as a benchmark reaction to test their catalytic capabilities. We consider both kinetic and thermodynamic factors that can influence the CO oxidation.

II. MODEL SYSTEM: Au_{10} AND TiO_2 (110) SURFACE

As mentioned above, low-energy isomers of both neutral Au_{10} and anionic Au_{10}^- exhibit diverse structures, as shown in Fig. 1. At the coupled cluster theory with single and double excitations including perturbative triple excitations [CCSD(T)] and with inclusion of basis-set superposition error correction, the predicted lowest-energy neutral and anionic Au_{10} cluster is the 2D isomer **A1** (or **B3**), which has a planar hexagonal structure with the D_{2h} point-group symmetry.[29] The **B3** isomer of Au_{10}^- has been detected in the photoelectron spectroscopy experiment.[31] The predicted two

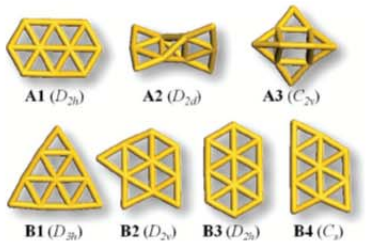

FIG. 1. Low-lying isomers of neutral (**A1–A3**; Refs. 28 and 29) and anionic (**B1–B4**; Ref. 31) Au_{10} cluster.

lowest-energy 3D isomers of neutral Au_{10} are **A2** (Ref. 28) and **A3**.[29] In our simulation, the planar **A1** isomer is chosen as the initial geometry prior to the collision because it is likely the global minimum for the neutral Au_{10}. To simulate an infinitely large TiO_2 (110) surface, the periodic boundary condition is used. Specifically, a supercell $(5\times2\times2)$ of 110-terminated rutile TiO_2, which contains 40 Ti atoms and 80 O atoms, is built as the oxide support. A vacuum space of 17 Å is set between the support and its images in the direction normal to the surface, which is sufficiently large to accommodate the Au_{10}. The starting position for the Au_{10}, measured from the Au atom nearest to the support, is 5.0 Å above the support.

The initial kinetic energy (E_k) of the gold cluster is a key factor that can influence the dynamic behavior of the cluster during the collision. In the soft-landing experiment, the impact kinetic energy E_k per atom is typically in the range of 0.1–1 eV,[21,22] which means that the impact velocity can be up to 10^3 m/s for the gold cluster. In this work, we considered two limiting cases for the initial velocity of the gold cluster: (1) 1000 m/s in the high-speed limit, which is very close to the speed involved in the soft-landing experiment, and (2) 100 m/s in the low-speed limit, which is close to the mean speed of free gold clusters in thermal motion. The direction of the impact velocity was set to be perpendicular to the support. Another important parameter that can significantly affect the dynamic behavior of the cluster during the collision is the relative orientation of the planar **A1** isomer with respect to the surface. In our simulation, again, we considered two limiting cases: one is that the long axis of **A1** is parallel to the surface normal (vertical collision), and another is that the plane of **A1** is parallel to the TiO_2 surface (parallel collision). In the simulation of the collision between **A1** and the defected TiO_2 surface, only the vertical collision in the high-speed scenario is considered, where the collision point is exactly at the site of oxygen vacancy.

III. COMPUTATIONAL DETAILS

The CPMD method based on the plane-wave density-functional theory (DFT) is employed, which is implemented in the CPMD 3.13.2 code.[32] Electronic structure calculations are carried out within the generalized gradient approximation with the Perdew–Burke–Ernzerhof exchange-correlation function.[33] The Goedecker norm-conserving pseudopotential[34,35] is used to model the interaction between

the valence electrons [$Au(5d^{10}6s^1)$, $Ti(3d^24s^2)$, and $O(2s^22p^4)$] and the atomic cores. The plane-wave energy cutoff is set to be 80 Ry for the wave functions. The electron surface potential (ESP) atomic charge analysis of the $[Au_{10}–TiO_2]^-$ system is performed using the REPEAT program developed by Campa *et al.*[36]

Both the geometries of the Au_{10} cluster and the TiO_2 (110) surface are optimized before the CPMD simulations. All the simulations are carried out in the *NVE* ensemble. The initial velocities of all atoms of the system are given according to the Boltzmann distribution at 298 K. Then these velocities are modified such that the relative velocity between the center of mass of **A1** and that of the TiO_2 substrate is equal to a predetermined collision velocity, v_c. The time step is set as 0.12 fs, and the total simulation times are 3.0 and 5.0 ps, respectively, for the high-speed and low-speed collision scenario. The CPMD simulations are performed using the supercomputer (Firefly) in University of Nebraska's Holland Computing Center.[37] 256 CPU cores are used for each CPMD simulation. The wall time of each ionic step is a little less than 40 s, and each CPMD simulation lasts about 20 days.

To assess the structure-activity relationship with the Au_{10} as the model catalyst, we compute the reaction pathways for the CO oxidation based on three low-energy isomer structures of Au_{10}: (1) the precollision 2D structure (**A1**), (2) a postcollision 3D structure (**A2**), and (3) a transient intermediate 3D structure during the collision (**A3**). For this computation, we used the Tao–Perdew–Staroverov–Scuseria (TPSS) (Ref. 38) functional and the 6-311+G(d) basis set for carbon and oxygen and the LANL2DZ effective core potential basis set[39] plus augmentation of two sets of *f* and one set of *g*-polarization function for gold (the exponents for *f* and *g* polarization functions are 1.424 69, 0.468 34, and 1.1469, respectively), as implemented in the GAUSSIAN 03 software package.[40] The good performance of TPSS functional for small gold cluster anions has been reported recently by Johansson *et al.*[38]

IV. RESULTS AND DISCUSSION

A. Simulation of the collision process

As mentioned above, because the global minimum of anionic cluster Au_{10}^- possesses 2D planar structures,[31] we select the **B3** (or **A1**) isomer as the initial precollision Au_{10}^- cluster. In fact, in all soft-landing experiments with gold clusters, the clusters must be either negatively or positively charged.[21,22] For example, in a recent soft-landing experiment of small-sized gold clusters, Au_{10} is negatively charged for mass selection.[21] When the Au_{10}^- is deposited on the TiO_2 substrate, it is possible that the negative charge is transferred to the TiO_2 substrate. To demonstrate this possibility, we first compute the ESP derived atomic charges for the $[Au_{10}–TiO_2]^-$ system, with or without an oxygen vacancy in the supercell (see Fig. 2). We find that the negative charge of the entire $[Au_{10}–TiO_2]^-$ system is mainly distributed on the TiO_2 substrate, with or without the oxygen vacancy. The

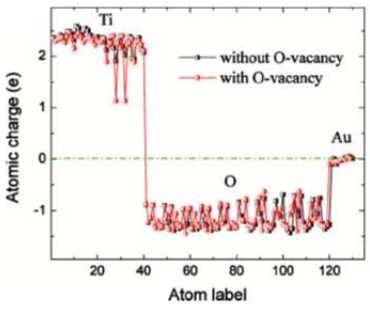

FIG. 2. Electron surface potential derived atomic charges of the $[Au_{10}–TiO_2]^-$ system with or without an oxygen defect. The black and red curves denote the perfect and defected TiO_2 (110) surface, respectively. The horizontal axis (atom label) refers to the total number of atoms in the supercell, which include 10 Au, 40 Ti, and 80 O.

gold cluster no longer carries any negative charge. Hence, during the collision, the negative charge on the Au_{10}^- cluster should be very likely transferred to the substrate and then redistributed over the entire (infinite) substrate. Indeed, several previous experimental studies have also shown that upon deposition of charged metal clusters, the clusters usually become neutralized.[22] Thus, we only perform the simulation on a neutral $[Au_{10}–TiO_2]$ system.

During the CPMD simulation, we record the time evolution of the temperature (computed from the average kinetic energy per ion) and the Kohn–Sham (KS) energy per supercell [see Figs. 3(a) and 3(b)]. The high-speed collision processes can be separated into three periods in time: precollision (0–0.3 ps), in the midst of the collision (0.3–0.9 ps), and postcollision (0.9–3 ps). In the first period, the **A1** isomer moves downward to the TiO_2 substrate, and the interaction

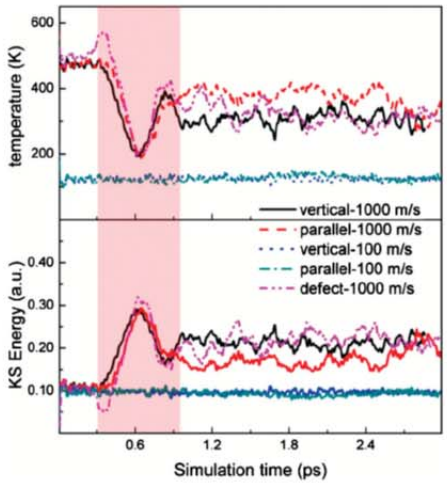

FIG. 3. (a) Temperature of the ions and (b) the Kohn–Sham energy per supercell in the course of the collision between the neutral Au_{10} and either a perfect TiO_2 (110) surface or the TiO_2 surface containing oxygen defects. In the high-speed (1000 m/s) case, the contact between the cluster (in either parallel or vertical orientation with respective to the TiO_2) and the surface occurs within the 0.3–0.9 ps period, highlighted by a shaded pink band.

between **A1** and the substrate is through the weak van der Waals interaction. Hence, both the temperature and the KS energy keep more or less constant. At the beginning of the second period, a significant decrease of temperature and an increase of KS energy can be observed (see black curve in Fig. 3), indicating that there is a substantial energy transfer from the kinetic energy to the KS energy when the collision starts. The kinetic energy reaches the lowest value at ~0.6 ps, where the system temperature decreases from ~500 to ~200 K, the relative velocity between the center of mass of the cluster and the TiO_2 is nearly zero, and the distance between the cluster and the TiO_2 is also the shortest. The simulation shows that about 5 eV of kinetic energy is transferred to the KS energy during the 0.3–0.6 ps period. The distribution of the transferred 5 eV energy between the cluster and the TiO_2 depends on the rigidity of the TiO_2 substrate. Since the Ti–O bonds (computed bond energy is ~6.8 eV) are relatively stronger than the Au–Au bonds (computed average bond energy is ~1.5 eV for the Au_{10}), the transferred kinetic energy is largely absorbed by the Au_{10}. The absorbed kinetic energy is redistributed within the Au_{10}, part of the energy is distributed back to the translation motion of the whole cluster, and another part is channeled into intracluster vibration and rotation. This latter energy gain by the cluster appears to be more than enough to overcome the deformation barrier of the Au_{10}, which results in the 2D-to-3D structural transition [see supplemental material movie S1 (Ref. 41) and Fig. 3(a)], thus confirming our speculation.

Beyond 0.6 ps, the Au_{10} starts to bounce back from the TiO_2, and the system temperature starts to increase again. In the 0.6–0.9 ps period, the KS energy is transferred back mainly to the ascending Au_{10} in the form of kinetic energy. Because the initial velocity of the cluster is high, the Au_{10} does not stick to the perfect TiO_2 surface after the collision. However, when the **A1** cluster collides with the defected TiO_2 (110) surface at the site of oxygen vacancy, a significant heat release can be detected in the beginning of the collision [see pink curve in Fig. 3(b)], suggesting the formation of a transient chemical bond at the site of oxygen vacancy during the collision. In the third period, the Au_{10} is far away enough from the TiO_2 to move freely. The KS energy in this period exhibits much larger fluctuation than that before the collision due to the transfer of a portion of kinetic energy to KS energy. There is an obviously small valley of the KS energy, concomitant with a small peak of temperature near 0.9 ps in the case of vertical collision (see black curve in Fig. 3), suggesting that the system just crosses over a transition barrier and arrives at a different isomeric structure.

Time-dependent temperature and KS energy of the system in the cases of low-speed collision are also displayed in Fig. 3. Because the initial kinetic energy is a hundredth of that in the high-speed collision, little change in the temperature and KS energy is observed (see blue curves in Fig. 3).

To gain more insight into the dynamics of the structural transition, snapshots of CPMD trajectories (supplemental material movie S1) of the **A1** cluster in several time stages during its collision with the TiO_2 (110) surface are shown in Fig. 4. The initial velocity (v_c) of **A1** in each simulation is

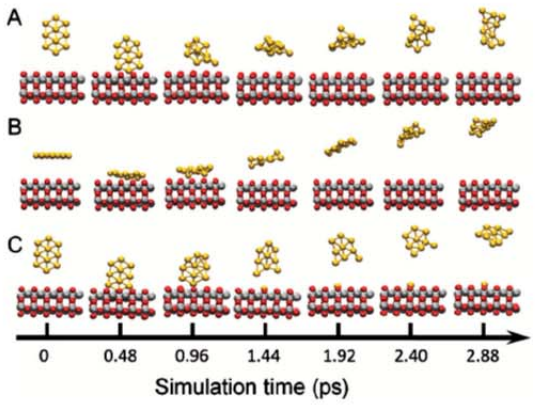

FIG. 4. Snapshots of the planar Au_{10} (**A1**) in collision with a TiO_2 (110) surface in several time stages of MD simulations, with the initial orientation of the **A1** being (a) perpendicular to and (b) parallel to a perfect TiO_2, and (c) perpendicular to a defected TiO_2 substrate, and located exactly on the top of the oxygen vacancy. The initial downward velocity of **A1** is 1000 m/s. Red spheres represent oxygen atoms and gray spheres represent Ti atoms.

1000 m/s. In the first case, the initial orientation of **A1** is perpendicular to the TiO_2 substrate [Fig. 4(a)], and a large structural deformation of **A1** during and after the collision can be observed. Specifically, within the time frame of 0.48–1.44 ps, the planar **A1** isomer folds when in close contact with the TiO_2, where the planar structure becomes a double-layer structure. More interestingly, at ~1.44 ps, a transient 3D isomer similar to **A3** can be observed. A geometry optimization of the transient structure (at 1.2 ps) gives exactly the **A3** isomer. Right after the collision, the isomer is still in a nonequilibrium state, evidenced by the larger fluctuation of the temperature. As such, the structure of the Au_{10} is still evolving until ~2.88 ps at which the transient structure becomes similar to the **A2** (postcollision) structure. Geometric optimization of this postcollision structure gives exactly the **A2** isomer. To our knowledge, this sequence of structural transitions from 2D to 3D during the soft landing has not been reported previously.

In contrast, no structural transition is observed when the initial orientation of the **A1** isomer is parallel to the TiO_2 [see supplemental material movie S2 (Ref. 41) and Fig. 4(b)]. Only modest structural deformation of **A1** is observed mainly in the postcollision period (e.g., from 1.44 to 2.88 ps). Beyond 2.88 ps, the **A1** isomer recovers so that the entire collision process essentially behaves like an elastic collision. The sharp contrast between the vertical and parallel collision can be understood on the basis of the following explanation: in the vertical collision scenario, only several Au atoms at the bottom of the cluster are in contact with the TiO_2 during the collision, but not in a simultaneous fashion. As such, when the bottom atoms have changed their velocity to the upward direction, atoms on the top of the **A1** isomer are still in the downward direction, which led to a large structural deformation. However, in the parallel collision scenario, all the Au atoms are in contact with the TiO_2 (110) surface almost simultaneously. Hence, only weak structural

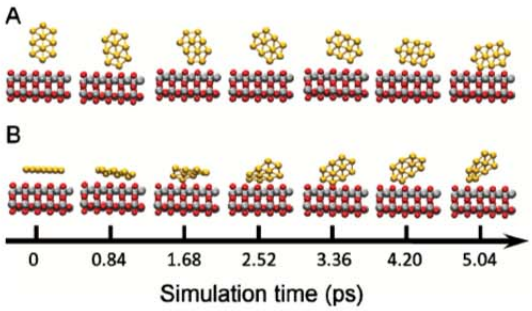

FIG. 5. Snapshots of the planar Au_{10} (**A1**) in collision with a perfect TiO_2 (110) surface in several time stages of MD simulations, with the initial orientation of Au_{10} being (a) perpendicular to and (b) parallel to the TiO_2 substrate. The initial downward velocity of **A1** is 100 m/s.

deformation is induced mainly by the local atomic structures of the TiO_2 (110) surface.

The collision between the **A1** isomer (initially in the vertical orientation) and the defected TiO_2 (110) surface with an oxygen vacancy (per supercell) exhibits a more interesting behavior [supplemental material movie S3 (Ref. 41) and Fig. 4(c)]. It turns out that one of Au atoms at the very bottom of the cluster is trapped by the oxygen vacancy when the remaining Au_9 cluster ascends after the collision. In other words, the Ti–Au bonds are formed during the collision [Fig. 4(c)], and these bonds are stronger than the Au–Au bonds. Hence, in the high-speed limit of the soft landing, the gold cluster may loss one Au if one of its atoms happens to be trapped by the oxygen vacancy.

Snapshots of CPMD trajectories in the cases of the low-speed limit for the soft landing (i.e., $v_c = 100$ m/s) are displayed in Fig. 5. Regardless of initial orientation of the **A1** isomer (either vertical or parallel), no distinctive structural transition is observed during the collision. More importantly, the **A1** isomer never detaches from the TiO_2 after the collision with the perfect TiO_2 substrate, nor stays in the same location due to relatively weak interaction between the cluster and the TiO_2. Rather, the **A1** isomer is tilted and undergoes a self-rotation on the TiO_2 after the cluster collides with the TiO_2 vertically [Fig. 5(a)]. In reality, the relaxation time for the cluster on the TiO_2 may be much longer than the 5 ps time scale discussed here. When the **A1** isomer collides with the perfect TiO_2 substrate parallelly [Fig. 5(b) and supplemental materials movie S4 (Ref. 41)], the cluster tends to have one Au atom in contact with the TiO_2. Hence, in the real-world experiment, the cluster may drift around on the substrate right after the collision and may be pinned down by an oxygen vacancy.

B. Reaction pathway for CO oxidation on three low-energy isomers of Au_{10}

In light of the sequence of structural transitions from 2D **A1** isomer to 3D isomers, **A3** and **A2** during the high-speed limit of the soft landing discussed above, we further examined the catalytic capability of these three low-lying isomers using the CO oxidation as a benchmark test. Two possible reaction pathways for the CO oxidation on these gold clusters are considered and depicted in Fig. 6: the Eley–Rideal (ER) and Langmuir–Hinshelwood (LH).[15–19,42–44] The LH pathway can be described as $CO_{(ads)} + O_{2(gas)} \rightarrow CO_{(ads)} + O_{2(ads)} \rightarrow OOCO_{(ads)} \rightarrow O_{(ads)} + CO_{2(gas)}$, and the ER pathway as $O_{2(gas)} + CO_{(gas)} \rightarrow O_{2(ads)} + CO_{(gas)} \rightarrow CO_{3(ads)} \rightarrow O_{(ads)} + CO_{2(gas)}$. The LH mechanism is initiated from coadsorption of CO and O_2, while in the ER mechanism O_2 is first activated into two atomic O by the gold cluster, followed by the attack of CO to an atomic O directly. Our DFT computation shows that adsorption energies of O_2 on the three isomers are all smaller in absolute value than −0.2 eV (here the more negative value means stronger adsorption). Because O_2 is very weakly adsorbed on the gold cluster, O_2 molecule cannot be dissociated into two atomic O. Hence, the ER pathway is unlikely. On the other hand, the adsorption energy of CO is about −1.0 eV, suggesting that the adsorption of CO should play a key role in the CO oxidation on the gold clusters. Hereafter, we only report the more likely LH reaction pathway.

The computed reaction pathway for the CO oxidation on **A1**, **A2** , and **A3** isomers is displayed in [Figs. 6(a)–6(c)], respectively. After the coadsorption of CO and O_2, the $Au_{10}-CO_3$ complex must cross two energy barriers to produce a gas molecule CO_2. As shown in Fig. 6, all three isomers exhibit high catalytic activity: For the planar **A1** isomer, the first energy barrier is 0.62 eV and the second is 0.42 eV. The higher adsorption energy of CO on the 3D **A2** isomer leads to a higher first barrier (0.78 eV) than that of **A1** or **A3**, but a lower second barrier (0.34 eV) than that of **A1** or **A3**. For the **A3** isomer, the first barrier is 0.67 eV, close to that on **A1**, while the second barrier (0.77 eV) is much higher than that on **A1** or **A2**. More interestingly, upon CO adsorption, the **A2** isomer undergoes major structural deformation [Fig. 6(b)], indicating that the 3D **A2** isomer is fairly fluxional. In fact, after the CO is oxidized, the planar **A1** isomer [Fig. 6(a)] and 3D **A3** isomer [Fig. 6(c)] remain intact while the **A2** isomer turns into a new structure [Fig. 6(b)]. Besides the reaction barrier, another important quantity for evaluating catalytic capability of gold cluster is the net heat release at the end of CO oxidation, which is −3.86 eV for **A2** and −3.78 eV for **A3**, both are much larger in value than that (−2.76 eV) for **A1**. Finally, the CO oxidation reaction involving the atomic O adsorbed on the gold cluster and a newly adsorbed CO from the gas phase is barrierless, as shown previously.[15]

V. CONCLUSION

In conclusion, we perform Car–Parrinello MD simulations to study the collision between a small-sized gold cluster Au_{10} and the TiO_2 (110) surface under two limiting conditions of the soft-landing experiment. The effects of the initial kinetic energy of the cluster, the initial orientation of the cluster with respect to the TiO_2 surface, as well as the oxygen vacancy on the TiO_2 surface on the dynamics and structure of the postcollision cluster are investigated. In the high-speed limit (1000 m/s) of the soft-landing, a sequence of structural transitions from the 2D **A1** isomer to the 3D **A2**

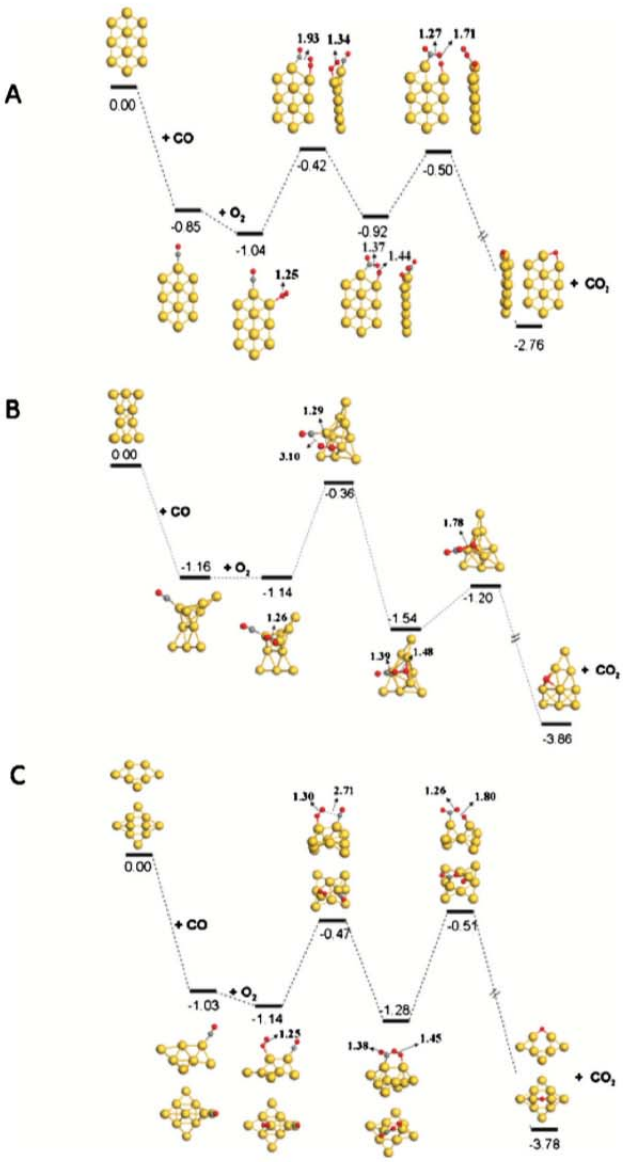

FIG. 6. Comparison of energy diagrams for the oxidation reaction CO $+O_2$! CO_2+O on three low-energy neutral Au_{10} isomers. Structures of the three isomers correspond to local minima of Au_{10} (a) before the collision (**A1** isomer), (b) after the collision (**A2**), and (c) in the midst of the collision (**A3**), respectively [see Fig. 4(a)]. The energies shown in the three reaction pathway diagrams are in eV, and the bond lengths marked on the gold clusters are in angstrom. In (c), both side and top views of the gold clusters are shown, while in (a) both side and top views of the gold clusters are shown in and beyond the first transition state.

and **A3** isomers is observed for the first time when **A1** is initially perpendicular to the perfect TiO_2 substrate. When **A1** is initially parallel to the perfect TiO_2 substrate, the collision between the **A1** isomer and the perfect TiO_2 (110) surface is akin to an elastic collision without showing any structural transition. On the other hand, in the low-speed limit (100 m/s) of the soft-landing, structural transitions are never observed regardless of the initial orientation of the cluster. When the TiO_2 (110) surface has oxygen vacancies, chemical bonds may form between Au and Ti atoms when the cluster is in contact with the vacancy. Still in the high-speed limit of the soft-landing, the oxygen vacancy is even capable of trapping an Au atom, thereby splitting the Au_{10} into two parts during the rebounding of the gold cluster from the support. Hence, if the TiO_2 substrate contains a lot of defects, the soft landing may result in some gold clusters losing a few Au atoms.

Finally, we examine the catalytic capability of both 2D and 3D isomers of Au_{10} using the CO oxidation as a benchmark test. We find that the CO oxidation on the planar **A1** isomer is kinetically more favorable than that on the 3D **A2** and **A3** isomers. However, the CO oxidation on **A2** and **A3** is thermodynamically more favorable than that on **A1**. Because the **A2** isomer is quite fluxional, its structure is unstable

against CO adsorption and can be easily transformed into a new 3D isomer structure upon the CO oxidation. Our results show clearly that a small-sized gold cluster with diverse isomer structures can entail rich catalytic behaviors, even if the support is an inert one.

ACKNOWLEDGMENTS

This work was supported by grants from NSF (Grant No. DMR-0820521), the Nebraska Research Initiative, and a seed grant by the Nebraska Center for Energy Sciences Research, and by the University of Nebraska's Holland Computing Center.

[1] M. Haruta, Catal. Today **36**, 153 (1997).
[2] M. Haruta and M. Date, Appl. Catal., A **222**, 427 (2001).
[3] M. Haruta, T. Kobayashi, H. Samo, and N. Yamada, Chem. Lett. **16**, 405 (1987).
[4] P. Schwerdtfeger, Angew. Chem., Int. Ed. **42**, 1892 (2003) and references cited therein.
[5] G. C. Bond, C. Louis, and D. T. Thompson, *Catalysis by Gold*, Catalytic Science Series Vol. 6 (Imperial College Press, London, 2006) and references therein.
[6] A. S. K. Hashmi and G. J. Hutchings, Angew. Chem., Int. Ed. **45**, 7896 (2006) and references therein.
[7] M. Chen and D. W. Goodman, Chem. Soc. Rev. **37**, 1860 (2008) and references therein.
[8] M. Valden, X. Lai, and D. W. Goodman, Science **281**, 1647 (1998).
[9] M. S. Chen and D. W. Goodman, Catal. Today **111**, 22 (2006) and references therein.
[10] Y. Iizuka, T. Tode, T. Takao, K. Yatsu, T. Takeuchi, S. Tsubota, and M. A. Haruta, J. Catal. **187**, 50 (1999).
[11] M. M. Schubert, S. Hackenberg, A. C. van Veen, M. Muhler, V. Plzak, and R. J. Behm, J. Catal. **197**, 113 (2001).
[12] J. Chou, N. R. Franklin, S. H. Baeck, T. F. Jaramillo, and E. W. McFarland, Catal. Lett. **95**, 107 (2004).
[13] S. H. Overbury, L. Ortiz-Soto, H. G. Zhu, B. Lee, M. D. Amiridis, and S. Dai, Catal. Lett. **95**, 99 (2004).
[14] R. J. H. Grisel and B. E. Nieuwenhuys, J. Catal. **199**, 48 (2001).
[15] A. Sanchez, S. Abbet, U. Heiz, W. D. Schneider, H. Hakkinen, R. N. Barnett, and U. Landman, J. Phys. Chem. A **103**, 9573 (1999).
[16] M. Mavrikakis, P. Stoltze, and J. K. Nørskov, Catal. Lett. **64**, 101 (2000).
[17] N. Lopez and J. K. Nørskov, Surf. Sci. **515**, 175 (2002).
[18] I. N. Remediakis, N. Lopez, and J. K. Nørskov, Angew. Chem., Int. Ed. **44**, 1824 (2005).
[19] N. Lopez and J. K. Nørskov, J. Am. Chem. Soc. **124**, 11262 (2002).
[20] M. Valden, S. Pak, X. Lai, and D. W. Goodman, Catal. Lett. **56**, 7 (1998).
[21] D. C. Lim, R. Dietsche, M. Bubek, G. Gantefor, and Y. D. Kim, ChemPhysChem **7**, 1909 (2006); R. Dietsche, D. C. Lim, M. Bubek, I. Lopez-Salido, G. Gantefoer, and Y. D. Kim, Appl. Phys. A: Mater. Sci. Process. **90**, 395 (2008).
[22] S. Vajda, R. E. Winans, J. W. Elam, B. Lee, M. J. Pellin, S. Seifert, G. Y. Tikhonov, and N. A. Tomczyk, Top. Catal. **39**, 161 (2006); S. Abbet, K. Judai, L. Klinger, and U. Heiz, Pure Appl. Chem. **74**, 1527 (2002); T. M. Bernhardt, U. Heiz, and U. Landman, *Nanocatalysis*, edited by U. Heiz and U. Landman (Springer-Verlag, Heidelberg, 2007) pp. 1–191.
[23] K. Bromann, H. Brune, C. F lix, W. Harbich, R. Monot, J. Buttet, and K. Kern, Surf. Sci. **377–379**, 1051 (1997).
[24] K. Kholmurodov, I. Puzynin, W. Smith, K. Yasuoka, and T. Ebisuzaki, Comput. Phys. Commun. **141**, 1 (2001).
[25] H. Rafii-Tabar, L. Jurczyszyn, and B. Stankiewicz, J. Phys.: Condens. Matter **12**, 5551 (2000).
[26] C. Zhang, A. Michaelides, D. A. King, and S. J. Jenkins, J. Am. Chem. Soc. **132**, 2175 (2010).
[27] A. Groß, Phys. Rev. Lett. **103**, 246101 (2009).
[28] B. Assadollahzadeh and P. Schwerdtfeger, J. Chem. Phys. **131**, 064306 (2009).
[29] Y. C. Choi, W. Y. Kim, H. M. Lee, and K. S. Kim, J. Chem. Theory Comput. **5**, 1216 (2009).
[30] H. H kkinen, B. Yoon, U. Landman, X. Li, H. J. Zhai, and L. S. Wang, J. Phys. Chem. A **107**, 6168 (2003).
[31] W. Huang and L. S. Wang, Phys. Chem. Chem. Phys. **11**, 2663 (2009); L. M. Wang, R. Pal, W. Huang, X. C. Zeng, and L. S. Wang, J. Chem. Phys. **132**, 114306 (2010).
[32] J. Hutter, A. Alavi, T. Deutsch, M. Bernasconi, S. Goedecker, D. Marx, M. Tuckerman, and M. Parrinello, CPMD, v3.13.2 (IBM Corp. and Max-Planck-Institut fuer Festkoerperforschung Stuttgart: 2009).
[33] J. P. Perdew, K. Burke, and M. Ernzerhof, Phys. Rev. Lett. **77**, 3865 (1996).
[34] S. Goedecker, M. Teter, and J. Hutter, Phys. Rev. B **54**, 1703 (1996).
[35] C. Hartwigsen, S. Goedecker, and J. Hutter, Phys. Rev. B **58**, 3641 (1998).
[36] C. Campa , B. Mussard, and T. K. Woo, J. Chem. Theory Comput. **5**, 2866 (2009).
[37] see http://hcc.unl.edu/.
[38] J. Tao, J. P. Perdew, V. N. Staroverov, and G. E. Scuseria, Phys. Rev. Lett. **91**, 146401 (2003); M. P. Johansson, A. Lechtken, D. Schooss, M. M. Kappes, and F. Furche, Phys. Rev. A **77**, 053202 (2008).
[39] P. J. Hay and W. R. Wadt, J. Chem. Phys. **82**, 270 (1985).
[40] M. J. Frisch, G. W. Trucks, H. B. Schlegel *et al.*, GAUSSIAN03, Revision E.01, Gaussian, Inc., Wallingford, CT, 2004.
[41] See supplementary material at http://dx.doi.org/10.1063/1.3485291 for more information of movie clips of quantum molecular dynamics simulations of collision between the gold cluster and TiO_2 substrate.
[42] W. An, Y. Pei, and X. C. Zeng, Nano Lett. **8**, 195 (2008).
[43] Y. Gao, N. Shao, S. Bulusu, and X. C. Zeng, J. Phys. Chem. C **112**, 8234 (2008); Y. Gao, N. Shao, Y. Pei, and X. C. Zeng, Nano Lett. **10**, 1055 (2010).
[44] H.-T. Chen, J.-G. Chang, S.-P. Ju, and H.-L. Chen, J. Comput. Chem. **31**, 258 (2010).